Excited-State Proton Transfer of 2-(2′-Pyridyl)benzimidazole in Microemulsions: Selective Enhancement and Slow Dynamics in Aerosol OT Reverse Micelles with an Aqueous Core

Tushar Kanti Mukherjee, Debashis Panda, and Anindya Datta*

Department of Chemistry, Indian Institute of Technology Bombay, Powai, Mumbai 400 076, India

Received: June 1, 2005; In Final Form: July 16, 2005

Excited-state proton transfer (ESPT) of 2-(2′-pyridyl)benzimidazole (2PBI) in reverse micelles has been studied by steady-state and time-resolved fluorescence spectroscopy. The nanometer sized water pool in the *n*-heptane/Aerosol OT (AOT)/water microemulsion is found to promote tautomer emission of this probe, as is evident from the emergence of a Stokes shifted band at 450 nm at the expense of the normal emission band on increasing the water content of the system. In the nonaquous microemulsion with a methanol core, the normal emission is quenched but no tautomer emission is obtained. With an acetonitrile core, there is no change in emission properties. Similarly, there is no evidence of ESPT in Triton X-100 reverse micelles. This indicates the requirement of ESPT to occur in microheterogeneous media; the medium should be a ternary system comprised of water and a hydrophobic phase separated by a negatively charged interface. In the microemulsions with an aqueous core, the fluorescence decays of 2PBI at the red end exhibit rise times of 0.8 ns and the time-resolved area-normalized emission spectra (TRANES) exhibit an isoemissive point, indicating slow dynamics of the two-state ESPT of 2PBI in aqueous AOT reverse micelles. The origin of the selective enhancement in AOT microemulsions as well as the slow dynamics is explored using fluorescence spectroscopic techniques, with support from quantum chemical calculation.

Introduction

Proton and hydrogen transfer reactions in the excited state have been studied extensively due to their numerous applications.[1−13] Excited-state proton transfer (ESPT) in hydrogen bonded systems such as benzimidazoles, in particular, has attracted a lot of attention.[5−9a] 2-(2′-Pyridyl)benzimidazole (2PBI) is a fluorophore that belongs to this class, the ESPT of the cationic form of which is manifested in a distinct dual emission in its aqueous solutions, in the pH range 3.5−0.5 (Scheme 1).[7] The inclusion of 2PBI in cyclodextrins hinders the solvent mediated ESPT to some extent due to a shielding of the fluorophore from water.[9a] Very recently, we reported that the ESPT of 2PBI is enhanced selectively in negatively charged sodium dodecyl sulfate (SDS) micelles at pH 7.[9c] This observation has been explained by a lower local pH at the micelle−water interface and a change in the pK_a of the fluorophore induced by the negatively charged micelle−water interface.[11] The dynamics of the proton transfer in SDS have been found to be slow, much like in several other excited-state processes where a slowing down occurs in restricted environments and is usually rationalized by the incomplete solvation of the transition state involved, leading to a higher barrier to the excited-state process.[10b,14] It is well-known that the solvation dynamics in bulk water is ultrafast, but over the past decade, there have been several reports of slow solvation dynamics in restricted environments, studied primarily by the time dependent Stokes shift of the emission spectra of fluorescent probes[14] and explained by a dynamic exchange between the bound as well as free water molecules present at the interface.[14f]

From our results on the ESPT of 2PBI in the micelle−water interface, we propose that the essential requirements for the observation of this phenomenon at pH 7 consist of water as a proton donor, a nonpolar phase, and a negatively charged interface between them. These requirements are fulfilled by the ternary *n*-heptane/Aerosol OT (AOT)/water microemulsions, where surfactant (AOT)-coated droplets of water are dispersed within an apolar phase. This system is suitable for a verification of our hypothesis, having the advantage of being well-characterized.[14−16] The water droplets in the microemulsions behave very differently from bulk water. They are known to have a lower polarity and exhibit slow solvation dynamics.[14] There have been several reports of excited-state proton transfer in AOT microemulsions.[16] In the present work, we have studied the occurrence of ESPT or lack thereof in microemulsions with aqueous and nonaqueous cores. Three different polar solvents have been chosen to form the core, namely, the polar protic water and methanol and polar aprotic acetonitrile, which is used to prepare a microemulsion devoid of specific hydrogen bonding

SCHEME 1: Solvent Mediated ESPT in 2PBI

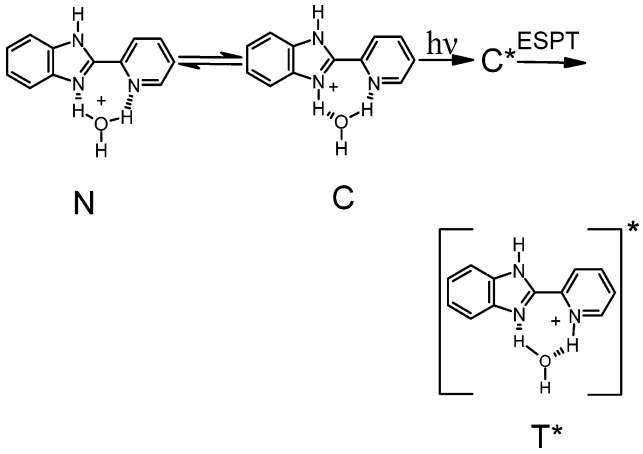

* To whom correspondence should be addresed. Phone: +91 22 2576 7149. Fax: +91 22 272 3480. E-mail: anindya@chem.iitb.ac.in.

10.1021/jp052917w CCC: $30.25
Published on Web 09/16/2005

interaction between the fluorophore and the solvent.[17] We have also performed the experiments in microemulsions of the neutral surfactant Triton X-100 (TX-100) in 30% benzene and 70% *n*-heptane, with a view to perform a control experiment in the absence of the high negative charge density present in AOT microemulsions. The shape, structure, and polarity of the TX-100 microemulsions are well-characterized, and thus, they provide an ideal system for our purposes.[18] The results of these experiments have been discussed with reference to the earlier results obtained in aqueous micelles and have been used to understand the phenomenon of ESPT of 2PBI in microheterogeneous media to a greater extent.

Experimental Section

2-(2′-Pyridyl)benzimidazole (AR grade) and Triton X-100 (TX-100) (AR grade) from Aldrich have been used as received. Aerosol OT from Aldrich is purified by the standard procedure.[14a,15f] The concentration of 2PBI used is 10 μM. The absorption spectra have been recorded on a JASCO V570 spectrophotometer with a 2 nm band-pass. Fluorescence spectra have been recorded on a Perkin-Elmer LS-55 spectrofluorimeter, with $\lambda_{ex} = 310$ nm. Time domain fluorescence data have been recorded on a TCSPC spectrometer, with $\lambda_{ex} = 286$ nm, obtained from the third harmonic of a mode-locked Ti:sapphire laser from Spectra Physics, U.S.A.[19a] The fluorescence decays have been collected with the emission polarizer at a magic angle of 54.7° and have been fitted to multiexponential functions after deconvolution using IBH DAS 6.0 software.[19b,c] To construct the time-resolved emission spectra (TRES), the fluorescence decays of 2PBI across the emission spectrum (350−500 nm) have been recorded at intervals of 10 nm. The fitted fluorescence decays have been scaled with the steady-state fluorescence intensities following the usual procedure. The spectra thus generated have been fitted to a sum of two Gaussian functions and are normalized to unit area to generate the time-resolved area-normalized emission spectra (TRANES).[9c,20]

Quantum chemical calculations have been performed using Gaussian 98.[21a] Density functional theory (DFT) and restricted Hartree−Fock (RHF) levels of theory have been used to obtain the ground-state geometries. Excited-state energies for these systems have been obtained using configuration interaction with single excitations (CIS) with the 6-31G* basis set.[21b,c] The structures are generated using Molkell.

Results

Absorption and Fluorescence Spectra. The absorption spectra of 2PBI in the reverse micelle, bulk water, and *n*-heptane are shown in Figure 1. In *n*-heptane, the spectrum is structured with bands at 311 and 326 nm (Figure 1e). In the presence of 0.1 M AOT, the spectrum does not change appreciably. With gradual addition of water, the spectrum becomes broader and less structured with the peak at 310 nm (Figure 1a). The excitation spectra are superimposable with the absorption spectra. The difference absorption spectra of 2PBI in the *n*-heptane/AOT/water microemulsion with 2PBI in *n*-heptane/AOT as the reference show a clear peak at 310 nm and a trough at 335 nm, which develops with gradual addition of water (Figure 1d). The changes in absorption spectra are not significant in the nonaqueous reverse micelles with methanol and acetonitrile cores (Figure 1b,c). The emission spectrum of 2PBI at $w_0 = 0$ is comprised of a single band at 360 nm, which is blue shifted with respect to 2PBI in water ($\lambda_{max} = 380$ nm) (Figure 2a).[7] With gradual addition of water, the intensity at the 360 nm band decreases and a new broad peak at 450 nm appears,

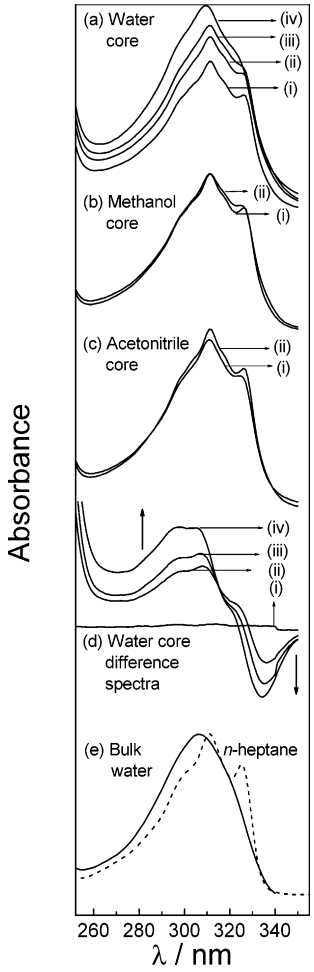

Figure 1. Absorption spectra of 2PBI in 0.1 M AOT reverse micelles in *n*-heptane with (a) a water core at different w_0 values of (i) 0, (ii) 4, (iii) 16, and (iv) 40; (b) a methanol core with *w* values of (i) 0 and (ii) 6; and (c) an acetonitrile core with *w* values of (i) 0 and (ii) 4. (d) Difference absorption spectra in the water nanopool at w_0 values of (i) 0, (ii) 4, (iii) 16, and (iv) 40. (e) Absorption spectra of 2PBI in bulk water (solid line) and *n*-heptane (dashed line).

with an isoemissive point at 414 nm. The spectra at the different water contents can be resolved into two components, one with a peak at ∼360 nm and the other with a peak at ∼450 nm. The spectrum at $w_0 = 40$ is depicted in Figure 3a, along with the components. A linear relationship is obtained by plotting the ratio of the fluorescence intensities at 450 and 360 nm against w_0 (Figure 3b). There is no change in the emission parameters in AOT microemulsions with an acetonitrile core (Figure 2c). The intensity of the 360 nm peak decreases gradually without the evolution of a Stokes shifted emission peak on addition of methanol in AOT microemulsions with a methanol core (Figure 2b). In the neutral Triton X-100 reverse micelles, addition of water has no significant effect on the emission spectrum with $\lambda_{max}^{em} = 350$ nm (Figure 2d).

Time-Resolved Studies and Quantum Chemical Calculations. The decay parameters of 2PBI in AOT reverse micelles are listed in Table 1. The decay times at $w_0 = 0$ are longer than those in bulk aqueous solution at pH 7.[9a,c] At $w_0 = 4$, the decay at 360 nm is much steeper and differs significantly from the decay profile at 450 nm. The notable changes are in the longer component at 360 nm and the shorter one at 450 nm, which change from 1.4 to 0.91 ns and 0.16 to 0.36, respectively, upon the first addition of water. The relative amplitudes of the shorter components at both of the wavelengths are found to increase as well. On further increase in water content ($w_0 = 4$ to 32),

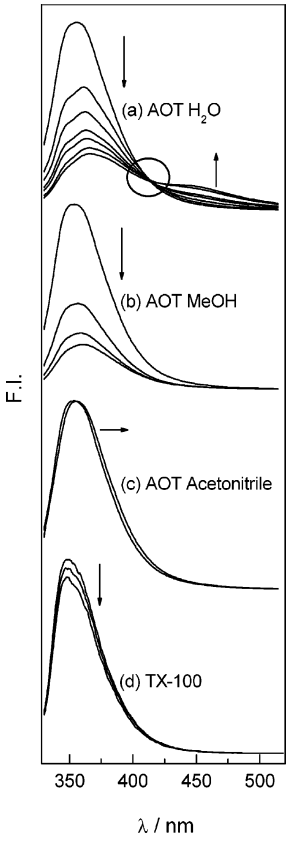

Figure 2. Fluorescence spectra of 2PBI in 0.1 M AOT microemulsions with cores of (a) water ($w_0 = 0$, 4, 8, 16, 24, 32, and 40), (b) methanol ($w = 0$, 2, 4, and 6), and (c) acetonitrile ($w = 0$ and 4). (d) Fluorescence spectra of 2PBI in Triton X-100 reverse micelles at ($w_0 = 0$, 5, and 9). The arrows indicate the increase in polar solvent contents. $\lambda_{ex} =$ 310 nm.

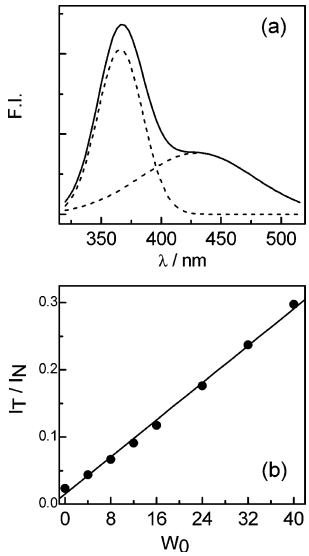

Figure 3. (a) Components of the fluorescence spectrum of 2PBI at $w_0 = 40$, with peaks at 360 and 450 nm. The experimentally obtained spectrum is shown by the solid line, and the components are shown by the dashed lines. (b) Variation of the ratio of the fluorescence intensities at 450 and 360 nm with water content.

the two components at 360 nm increase slightly from 0.17 to 0.22 ns and from 0.91 to 0.98 ns, with the amplitudes becoming equal. At 450 nm, the longer component increases from 1.61 to 3.88 ns, whereas the shorter component decreases progressively in value as well as amplitude, until a rise time of 0.80 ns is observed at $w_0 = 32$. Time-resolved emission spectra (TRES)

TABLE 1: Temporal Characteristics of Fluorescence of 2PBI in 0.1 M AOT Microemulsions with an Aqueous Core as a Function of Water Content[a]

	360 nm					450 nm				
w_0	τ_1	τ_2	a_1	a_2	χ^2	τ_1	τ_2	a_1	a_2	χ^2
0	0.17	1.4	0.27	0.73	1.11	0.17	1.66	0.22	0.78	1.14
4	0.19	0.91	0.38	0.62	1.10	0.36	1.61	0.39	0.61	1.17
12	0.19	0.94	0.47	0.53	1.13	0.29	3.35	0.48	0.52	1.11
24	0.22	0.95	0.51	0.49	1.15	0.21	3.70	0.35	0.65	1.10
32	0.22	0.98	0.52	0.48	1.04	0.80	3.88	−0.10	1.10	1.12

[a] The lifetimes are in nanoseconds.

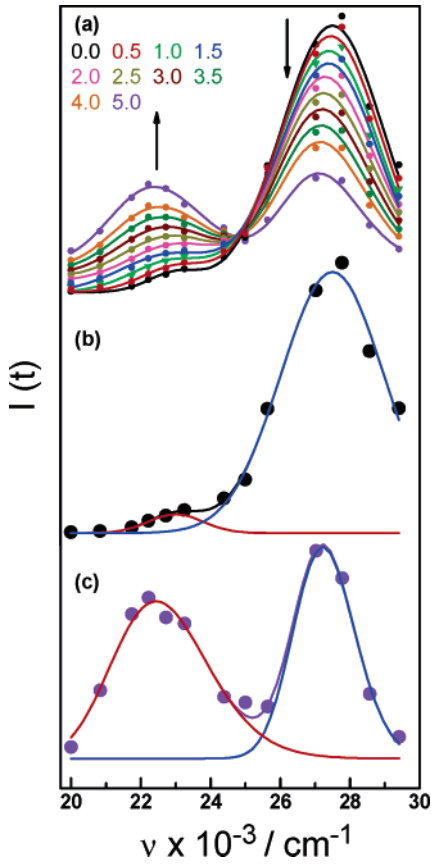

Figure 4. (a) Representative time-resolved area-normalized emission spectra (TRANES) of 2PBI in 0.1 M AOT reverse micelles at $w_0 =$ 32, between time 0 and 5.0 ns, and the components of TRANES at time (b) 0 ns and (c) 5.0 ns after excitation. The fits are shown by solid black lines in (b) and solid blue line in (c), and the components are shown by blue and red lines.

and time-resolved area-normalized emission spectra (TRANES) at $w_0 = 32$ have been constructed using the fluorescence decays recorded in the range 340−500 nm at 10 nm intervals. The TRANES pass through an isoemissive point at 24 781 cm^{-1} (Figure 4a).

The geometry-optimized structures of the normal, cationic, and tautomer forms are shown in Figure 6. The energies and dipole moments are listed in Table 2. It is noteworthy that even though the energies of the C* and T* forms are comparable, T* has a much greater dipole moment than C*.

Discussion

The spectral broadening and loss of structural features on addition of water to AOT in *n*-heptane indicates that 2PBI experiences a more polar environment compared to $w_0 = 0$, which is expected to happen if the chromophore molecules move from a nonpolar to a polar region (Figure 1a). This migration

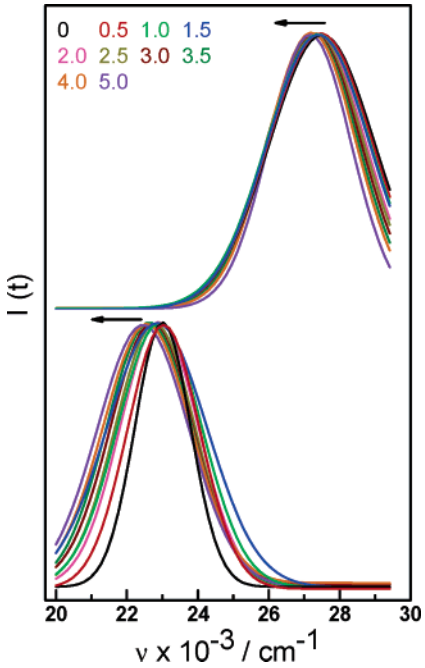

Figure 5. Time evolution of emission spectra. The upper panel contains the peak-normalized components of time-resolved emission spectra of 2PBI in 0.1 M AOT reverse micelles in the region of normal emission, and the lower panel contains those in the region of tautomer emission. The times are 0, 0.5, 1.0, 1.5, 2.0, 2.5, 3.0, 3.5, 4.0, and 5.0 ns in all cases. The spectra move toward lower energies with the passage of time.

TABLE 2: Energies and Dipole Moments of the Normal, Cationic, and Tautomeric Forms of 2PBI[a]

		B3LYP/ 6-31G*	B3LYP/ 6-311G**	RHF/ 6-31G*	CIS/ 6-31G*
N	energy	−1 646 080	−1 646 480	−1 635 740	
	dipole moment	4.83	4.86	5.12	
C	energy	−1 647 150	−1 647 530	−1 636 810	−1 636 760
	dipole moment	1.97	2.01	2.35	2.74
T	energy	−1 647 120	−1 647 510	−1 636 770	−1 636 740
	dipole moment	7.17	7.23	9.15	7.9

[a] The units of energy and dipole moment are kilojoules per mole and debyes, respectively.

is highlighted more prominently in the difference absorption spectra (Figure 1d). With an increase in the size of the water pool, a peak grows at 310 nm and a trough develops at 335 nm (Figure 1d), indicating a transfer of population of 2PBI molecules into the water pool, as the trough develops in the region where 2PBI in *n*-heptane has a relatively greater absorbance than water and the peak comes up in the region where the absorbance in water is relatively larger (Figure 1e). This is reminiscent of the earlier observations of nile red in AOT reverse micelles.[15f] The insignificant spectral changes in the polar aprotic core of acetonitrile, nonaqueous polar protic core of methanol, and TX-100 reverse micelles with an aqueous core indicate that there is some kind of a specific interaction of 2PBI with the water molecules in AOT reverse micelles with an aqueous core. The selective change in environment in the AOT microemulsion with an aqueous core becomes even more evident in the emission spectra (Figure 2). A notable decrease in the 360 nm peak accompanied by the development of the Stokes shifted emission peak at 450 nm is observed only in AOT reverse micelles with an aqueous core and not in the other three reverse micellar systems studied. An isoemissive point in the fluorescence spectra of 2PBI in the *n*-heptane/AOT/water microemulsion indicates that the two emitting species are in

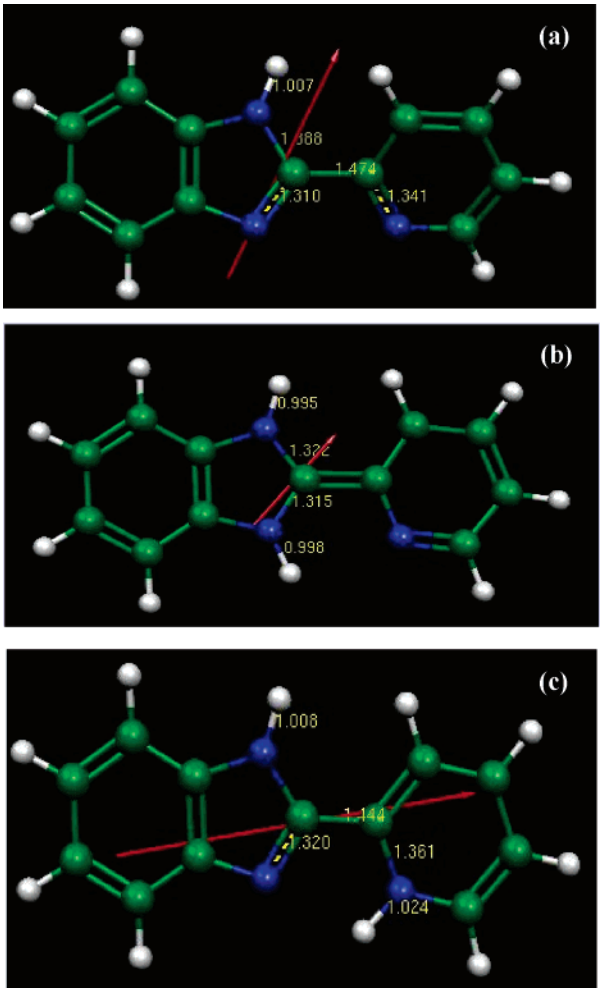

Figure 6. Geometry-optimized structures of (a) the neutral form, (b) the cationic form, and (c) the tautomer form of 2PBI with 6-31G* basis sets. The red arrow indicates the magnitude and direction of the dipole moment.

dynamic equilibrium. The Stokes shifted emission peak, the intensity of which increases linearly with the size of the water pool (w_0) is due to the emission from the tautomeric form of 2PBI.[7,9] Its emergence in the aqueous AOT microemulsions substantiates our hypothesis that the essential requirements for ESPT in microheterogeneous media are water, a nonpolar phase, and a negatively charged boundary that separates them. Among the systems under investigation, all three criteria are met only in the AOT microemulsions with an aqueous core. The lack of ESPT in reverse micelles with an acetonitrile core is understandable, since, in this case, there is no proton donor. Methanol is known to quench the normal emission in its mixtures with heptane, due to the formation of nonemissive hydrogen bonded complexes with methanol.[8b] The selective promotion of ESPT in the water/AOT/*n*-heptane system can be explained in a similar manner as in the case of aqueous SDS micelles, as is discussed in the next paragraph.

Previously, we reported a selective enhancement of ESPT of 2PBI at neutral pH 7 by negatively charged SDS micelles.[9c] This was rationalized by the consideration of two factors: modification of the pK_a of 2PBI at the micelle−water interface and a lower local pH at the interface. It is well-known that the local pH of the Stern layer of SDS micelles is less than 7, as the hydronium ions of water are attracted toward the negatively charged Stern layer and are distributed to a greater extent in the vicinity of this layer.[10b,11a,c] The present situation is rather

similar. AOT reverse micelles have an inverted spherical structure with negatively charged sulfonate groups (SO_3^-) facing the polar solvents. The pH of the water molecules associated with the sulfonate groups in the nanocavity is less than the bulk pH, as the hydronium ions of water are attracted toward the negatively charged sulfonate groups similar to the case of SDS micelles.[11b] The increased local acidity can cause the protonation of 2PBI in the interfacial region, and the cations thus formed can undergo ESPT to give rise to the tautomer emission (Scheme 1). This mechanism can be ruled out for the Triton X-100 and nonaqueous (methanol and acetonitrile) AOT reverse micelles, and this explains the absence of dual emission in them. Another factor that could be of profound importance is the stabilization of the cationic form by the negatively charged interface, as has been observed in 4-methyl-7-hydroxyflavylium chloride by Quina and co-workers.[11c] It is possible that the protonated form (C) of 2PBI that is formed with the abstraction of a proton from the water molecules in the water pool is stabilized by electrostatic attraction by the negatively charged headgroups of AOT, and thus, the relative population of C increases, leading to a greater extent of ESPT as the water content increases. This is reminiscent of the internal Stark effect obtained by Klymchenko and Demchenko in 3-hydroxyflavone derivatives.[2a]

The time-resolved fluorescence data afford additional evidence for the inferences drawn from the steady-state experiment, over and above providing some insight into the dynamics of the photoprocesses involved. The shorter lifetime of 0.17 ns at 360 nm obtained for $w_0 = 0$ is very close to that reported earlier for the neutral form (N*) of 2PBI in methanol, ethanol, and 2-propanol. The long component, on the other hand, matches the lifetime in nonpolar solvents.[8b] The 0.17 ns component is present at 450 nm as well. From the time-resolved data, it appears that the emission is almost entirely due to N* in two kinds of environments: first, the apolar solvent and the hydrophobic tail of AOT, and second, the ionic headgroup region. The 1.66 ns component could result from N* in the apolar region as well as C* that might be formed to a small extent in the headgroup region. It should be noted that the emission from C*, at 450 nm, has been earlier associated with a lifetime of 1.8 ns in water.[9c] It is known that, even at $w_0 = 0$, minute amounts of water are present in AOT reverse micelles and this water might cause the formation of C* to some extent.[15e]

The time constant associated with N* emission in the interfacial region at 360 nm increases to a small extent upon further addition of water. A more significant increase is obtained in its relative amplitude, which saturates at $w_0 = 24$. This would indicate an increase in the concentration of the neutral species in the headgroup region, which is in agreement with the absorption results. The contention about transfer of population from the apolar region to the headgroups and the water pool gains further support from the fact that the time constant of 1.4 ns, associated with emission from N* in apolar regions, gives way to that of ~0.9 ns, which is close to that of C* emission in the micellar interfacial region.[9c] Thus, we find that, on increasing the water content, not only do the 2PBI molecules get transferred to the interface and the aqueous core of the microemulsions, but they also undergo protonation. Notably, the relative amplitude of the C* emission decreases as the water content increases. This could be due to phototautomerization, which increases with water content, as is evident from the steady-state spectra.

The 450 nm emission is predominantly from the phototautomer (T*), but there are contributions from the tails of the emission from N* and C* as well. Consequently, the assignment of time constants at intermediate w_0 values is not very straightforward, especially as there is a possibility of diffusion of the fluorophores from one compartment to the other. However, at the highest water content, where the T* emission is very strong, there is a distinct growth in the red end, along with a decay of 3.88 ns, which is close to that associated with T* emission in the micellar interfacial region.[9c] It may be tempting to associate this growth with the time associated with the ESPT process, but it should be remembered that, in a microheterogeneous system like AOT microemulsion, the ESPT is not expected to be a purely two-state process, as solvation takes place in slower time scales in these media and this provides a competing pathway through which the rise time can occur.[14] Moreover, the slow and incomplete solvation can cause a smaller lowering of the energy barrier of the photoprocess, thereby slowing it down. To explore the different origins of the long rise time in AOT microemulsions with an aqueous core, we have performed a time-resolved area-normalized emission spectroscopic analysis of the data. Periasamy and co-workers have developed this technique and have established that an isoemissive point in TRANES indicates the presence of two distinct emissive species.[20] In the present study, the TRANES of 2PBI in AOT reverse micelles at $w_0 = 32$ exhibit two prominent peaks in the region of the normal and tautomer emission. A clear isoemissive point is obtained at 24 781 cm^{-1} (Figure 4a). The spectra can be resolved into two components, the redder one of which can be assigned to the tautomer emission. Representative spectra at 0 and 5 ns after excitation are shown in parts b and c of Figure 4, respectively, along with the components. With the passage of time, the band at 22 309 cm^{-1} is clearly seen to grow at the expense of the one at 27 387 cm^{-1}. Since the component at the lower energy grows from that at the higher energy, they can be ascribed to the emissions from the tautomeric and the cationic excited states, respectively. A small time dependent Stokes shift (TDSS) is observed for the cationic emission over a period of 5 ns (Figure 5, upper panel), while the TDSS of the tautomer peak is quite significant (Figure 5, lower panel). This is clearly a signature of dynamic solvation of the tautomeric form (T*) after it is formed by the ESPT process. Thus, some amount of the rise time observed at 450 nm must be due to the slow solvation of T*. To explain the slower solvation dynamics of the tautomeric form of 2PBI compared with the normal form, we have optimized the geometries of the ground state and have computed the energies and dipole moments of the cationic form (C) and its tautomeric form (T) in the ground state (S_0) as well as in the first excited singlet state (S_1) (Figure 6). The value of the computed ground-state dipole moment of the cationic form is 2.0 D, whereas that for its excited state is 2.7 D. The dipole moment of the tautomer in the excited state is much higher (7.9 D) (Table 2, Scheme 2). On going from the cationic form (C) to the tautomer form (T*), the direction of the dipole moment changes. These two factors can contribute to the slow solvation dynamics of 2PBI in restricted environments of micelles and reverse micelles.

It should be noted here that the intensity of the tautomer band at time zero is small but significant (Figure 4b). Thus, some amount of ESPT occurs within the zero time of our experiment or, in other words, some amount of the ultrafast component of ESPT is present in reverse micelles, like in SDS micellar solutions. Of course, the mechanism involving the slowing down of the ESPT process itself is also operative, as the TRANES in the time range 0−5.0 ns show an isoemissive point, indicating that the ESPT from the cationic to the tautomeric species is in progress in this time range as well. Thus, we find that the

SCHEME 2: Energy Levels Involved in the ESPT Process and Their Lifetimes in Aerosol OT Microemulsions

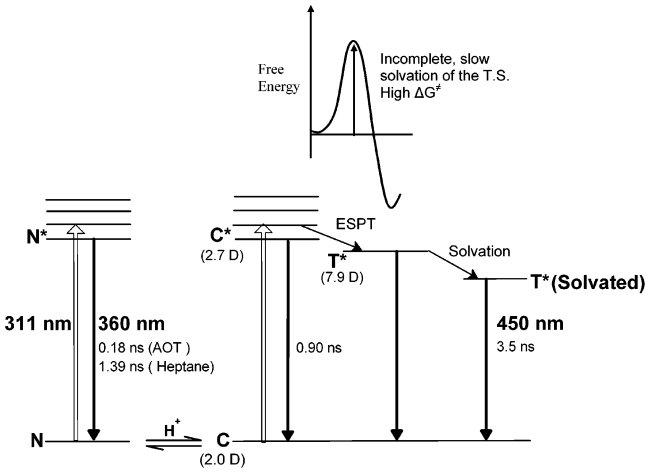

TRANES analysis of the data indicates that the rise time of the tautomer emission is most likely to be a convolution of both of the mechanisms discussed above, much like that observed in aqueous SDS micelles.

Conclusion

The enhancement and slow dynamics of the tautomer emission of 2PBI in AOT microemulsions with an aqueous core is observed, much like that observed in aqueous SDS micelles. The rise time observed in the tautomer emission is explained by consideration of slowing down of the ESPT process and slow solvation of the more polar excited state of the tautomeric form in the restricted environment of the microemulsion. The results and these discussions are summarized in Scheme 2. The selective occurrence of ESPT in the AOT microemulsion with an aqueous core and its absence in the nonaqueous and Triton X-100 microemulsions lend support to our contention that ESPT in 2PBI can be brought about in microheterogeneous syatems comprised of water and an apolar phase separated by a negatively charged boundary. The cause of the enhancement in aqueous AOT microemulsions can be ascribed to the formation of the cationic form in this system and also its stabilization due to favorable electrostatic interactions with the negatively charged headgroups of AOT. Another possible reason could be the local pH that is lower than 7. This could have rather important implications in the application of 2PBI in analytical biochemistry. First, it could be used as a fluorescent sensor for local pH. Second, it might have future applications in microscopy and imaging. As the normal emission arises mainly from the bulk solvent and the tautomer emission arises mainly at the negatively charged interface, they can be used for microscopic imaging of the cytoplasm and the cell membrane, respectively. The principal problem that might arise in such applications is the absorption of the fluorophore in the ultraviolet range. However, this problem can be circumvented by using multiphoton excitation. Further experiments in fluorescence dynamics and confocal microscopy are in progress to explore this possibility to a greater extent.

Acknowledgment. This work is supported by CSIR research grant no. 01 (1851)/03/EMR-II. T.K.M. and D.P. thank University Grants Commission, India, and CSIR, India, respectively, for Junior Research Fellowships. The authors are thankful to Prof. P. Ramamurthy and Ms. Indirapriyadharshini V. K. at National Centre for Ultrafast Processes, University of Madras, for the lifetime measurements. Thanks are due to Prof. G. K. Lahiri for the kind gift of 2PBI and numerous useful discussions.

References and Notes

(1) (a) Catalan, J.; Perez, P.; Del Valle, J. C.; de Paz, J. L. G.; Kasha, M. *Proc. Natl. Acad. Sci. U.S.A.* **2004**, *101*, 419. (b) Catalan, J.; Perez, P. *Phys. Chem. Chem. Phys.* **2005**, *7*, 94. (c) Agmon, N. *J. Phys. Chem. A* **2005**, *109*, 13.

(2) (a) Klymchenko, A. S.; Demchenko, A. P. *J. Am. Chem. Soc.* **2002**, *124*, 12372. (b) Schultz, T.; Samoylova, E.; Radloff, W.; Hertel, I. V.; Sobolewski, A. L.; Domcke, W. *Science* **2004**, *306*, 1765.

(3) (a) Kosower, E. M.; Huppert, D. *Annu. Rev. Phys. Chem.* **1986**, *37*, 127. (b) Petrich, J. W. *Int. Rev. Phys. Chem.* **2000**, *19*, 479. (c) Douhal, A.; Lahmani, F.; Zehnacker-Rentien, A.; Amat-Guerri, F. *J. Phys. Chem.* **1994**, *98*, 12198. (d) Abou El-Nasr, E. A.; Fujii, A.; Yahagi, T.; Ebata, T.; Mikami, N. *J. Phys. Chem. A* **2005**, *109*, 2498.

(4) (a) Smith, T. P.; Zaklika, K. A.; Thakur, K.; Walker, G. C.; Tominaga, K.; Barbara, P. F. *J. Phys. Chem.* **1991**, *95*, 10465. (b) Pfeiffer, M.; Lau, A.; Lenz, K.; Elsaesser, T. *Chem. Phys. Lett.* **1997**, *268*, 258. (c) Takeuchi, S.; Tahara, T. *Chem. Phys. Lett.* **2001**, *347*, 108.

(5) (a) Rios, M. A.; Rios, M. C. *J. Phys. Chem. A* **1998**, *102*, 1560. (b) Fahrni, C. J.; Henary, M. M.; Van Derveer, D. G. *J. Phys. Chem. A* **2002**, *106*, 7655. (c) Catalan, J.; De Paz, J. L. G.; Del Valle, J. C.; Claramunt, R. M.; Mas, Th. *Chem. Phys.* **2004**, *305*, 175.

(6) (a) Rodríguez, M. C.; Penedo, J. C.; Willemse, R. J.; Mosquera, M.; Rodríguez-Prieto, F. *J. Phys. Chem. A* **1999**, *103*, 7236. (b) Penedo, J. C.; Mosquera, M.; Rodríguez-Prieto, F. *J. Phys. Chem. A* **2000**, *104*, 7429. (c) Penedo, J. C.; Lustres, J. L. P.; Lema, I. G.; Rodríguez, M. C. R.; Mosquera, M.; Rodríguez-Prieto, F. *J. Phys. Chem. A* **2004**, *108*, 6117.

(7) (a) Rodríguez-Prieto, F.; Mosquera, M.; Novo, M. *J. Phys. Chem.* **1990**, *94*, 8536. (b) Novo, M.; Mosquera, M.; Rodríguez-Prieto, F. *Can. J. Chem.* **1992**, *70*, 823. (c) Novo, M.; Mosquera, M.; Rodríguez-Prieto, F. *J. Chem. Soc., Faraday Trans. 2* **1993**, *89*, 885. (d) Novo, M.; Mosquera, M.; Rodríguez-Prieto, F. *J. Phys. Chem.* **1995**, *99*, 14726.

(8) (a) Kondo, M. *Bull. Chem. Soc. Jpn.* **1978**, *51*, 3027. (b) Brown, R. G.; Entwistle, N.; Hepworth, J. D.; Hodgson, K. W.; May, B. *J. Phys. Chem.* **1982**, *86*, 2418.

(9) (a) Rath, M. C.; Palit, D. K.; Mukherjee, T. *J. Chem. Soc., Faraday Trans.* **1998**, *94*, 1189. (b) Douhal, A.; Fiebig, T.; Chachisvilis, M.; Zewail, A. H. *J. Phys. Chem. A* **1998**, *102*, 1657. (c) Mukherjee, T. K.; Ahuja, P.; Koner, A. L.; Datta, A. *J. Phys. Chem. B* **2005**, *109*, 12567.

(10) (a) Sarkar, N.; Das, K.; Das, S.; Datta, A.; Nath, D. N.; Bhattacharyya, K. *J. Phys. Chem.* **1995**, *99*, 17711. (b) Roy, D.; Karmakar, R.; Mondal, S. K.; Sahu, K.; Bhattacharyya, K. *Chem. Phys. Lett.* **2004**, *399*, 147.

(11) (a) Bunton, C. A.; Nome, F. J.; Quina, F. H.; Romsted, L. S. *Acc. Chem. Res.* **1991**, *24*, 357. (b) Pal, S. K.; Mandal, D.; Bhattacharyya, K. *J. Phys. Chem. B* **1998**, *102*, 11017. (c) Giestas, L.; Yihwa, C.; Lima, J. C.; Vautier-Giongo, C.; Lopes, A.; Macanita, A. L.; Quina, F. H. *J. Phys. Chem. A* **2003**, *107*, 3263.

(12) (a) Bardez, E.; Monnier, E.; Valeur, B. *J. Phys. Chem.* **1985**, *89*, 5031. (b) GuhaRoy, J.; Sengupta, P. K. *Chem. Phys. Lett.* **1994**, *230*, 75. (c) Andrade, S. M.; Costa, S. M. B.; Pansu, R. *Photochem. Photobiol.* **2000**, *71*, 405. (d) Cohen, B.; Huppert, D.; Solntsev, K. M.; Tsfadia, Y.; Nachliel, E.; Gutman, M. *J. Am. Chem. Soc.* **2002**, *124*, 7539.

(13) (a) Klymchenko, A. S.; Duportail, G.; Mely, Y.; Demchenko, A. P. *Proc. Natl. Acad. Sci. U.S.A.* **2003**, *100*, 11219. (b) Klymchenko, A. S.; Duportail, G.; Demchenko, A. P.; Mely, Y. *Biophys. J.* **2004**, *86*, 2929.

(14) (a) Wong, M.; Thomas, J. K.; Graetzel, M. *J. Am. Chem. Soc.* **1976**, *98*, 2391. (b) Belletete, M.; Lachapelle, M.; Durocher, G. *J. Phys. Chem.* **1990**, *94*, 5337. (c) Das, S.; Datta, A.; Bhattacharyya, K. *J. Phys. Chem. A* **1997**, *101*, 3299. (d) Riter, R. E.; Willard, D. M.; Levinger, N. E. *J. Phys. Chem. B* **1998**, *102*, 2705. (e) Nandi, N.; Bhattacharyya, K.; Bagchi, B. *Chem. Rev.* **2000**, *100*, 2013. (f) Pal, S.; Balasubramanian, S.; Bagchi, B. *Phys. Rev. Lett.* **2002**, *89*, 115505.

(15) (a) Luisi, P. L. *Angew Chem., Int. Ed. Engl.* **1985**, *97*, 449. (b) Langevin, D. *Acc. Chem. Res.* **1988**, *21*, 255. (c) Jain, T. K.; Varshney, M.; Maitra, A. *J. Phys. Chem.* **1989**, *93*, 7409. (d) Cho, C. H.; Chung, M.; Lee, J.; Nguyen, T.; Singh, S.; Vedamuthu, M.; Yao, S.; Zhu, J.-B.; Robinson, G. W. *J. Phys. Chem.* **1995**, *99*, 7806. (e) Moulik, S. P.; Mukherjee, K. *Proc. Indian Natl. Sci. Acad., Part A* **1996**, *62*, 215. (f) Datta, A.; Mandal, D.; Pal, S. K.; Bhattacharyya, K. *J. Phys. Chem. B* **1997**, *101*, 10221.

(16) (a) Escabi-Perez, J. R.; Fendler, J. H. *J. Am. Chem. Soc.* **1978**, *100*, 2234. (b) Sarkar, M.; GuhaRay, J.; Sengupta, P. K. *Spectrochim. Acta, Part A* **1996**, *52*, 275. (c) Kwon, O. H.; Jang, D. J. *J. Phys. Chem. B* **2005**, *109*, 8049.

(17) (a) Riter, R. E.; Kimmel, J. R.; Undiks, E. P.; Levinger, N. E. *J. Phys. Chem. B* **1997**, *101*, 8292. (b) Riter, R. E.; Undiks, E. P.; Kimmel, J. R.; Levinger, N. E. *J. Phys. Chem. B* **1998**, *102*, 7931. (c) Shirota, H.;

Horie, K. *J. Phys. Chem. B* **1999**, *103*, 1437. (d) Hazra, P.; Chakrabarty, D.; Sarkar, N. *Langmuir* **2002**, *18*, 7872.

(18) (a) Zhu, D.-M.; Wu, X.; Schelly, Z. A. *J. Phys. Chem.* **1992**, *96*, 7121. (b) Mandal, D.; Datta, A.; Pal, S. K.; Bhattacharyya, K. *J. Phys. Chem. B* **1998**, *102*, 9070. (c) Das, K.; Jain, B.; Patel, H. S. *Spectrochim. Acta, Part A* **2004**, *60*, 2059.

(19) (a) Thiagrajan, V.; Selvaraju, C.; Padma Malhar, E. J.; Ramamurthy, P. *ChemPhysChem* **2004**, *5*, 1200. (b) Mishra, P. P.; Koner, A. L.; Datta, A. *Chem. Phys. Lett.* **2004**, *400*, 128. (c) Mukherjee, T. K.; Mishra, P. P.; Datta, A. *Chem. Phys. Lett.* **2005**, *407*, 119.

(20) (a) Koti, A. S. R.; Krishna, M. M. G.; Periasamy, N. *J. Phys. Chem. A* **2001**, *105*, 1767. (b) Koti, A. S. R.; Periasamy, N. *Proc.−Indian Acad. Sci., Chem. Sci.* **2001**, *113*, 157. (c) Koti, A. S. R.; Periasamy, N. *J. Chem. Phys*. **2001**, *115*, 7094. (d) Maciejewski, A.; Kubicki, J.; Dobek, K. *J. Phys. Chem. B* **2003**, *107*, 13986.

(21) (a) Frisch, M. J.; Trucks, G. W.; Schlegel, H. B.; Scuseria, G. E.; Robb, M. A.; Cheeseman, J. R.; Zakrzewski, V. G.; Montgomery, J. A., Jr.; Stratmann, R. E.; Burant, J. C.; Dapprich, S.; Millam, J. M.; Daniels, A. D.; Kudin, K. N.; Strain, M. C.; Farkas, O.; Tomasi, J.; Barone, V.; Cossi, M.; Cammi, R.; Mennucci, B.; Pomelli, C.; Adamo, C.; Clifford, S.; Ochterski, J.; Petersson, G. A.; Ayala, P. Y.; Cui, Q.; Morokuma, K.; Malick, D. K.; Rabuck, A. D.; Raghavachari, K.; Foresman, J. B.; Cioslowski, J.; Ortiz, J. V.; Stefanov, B. B.; Liu, G.; Liashenko, A.; Piskorz, P.; Komaromi, I.; Gomperts, R.; Martin, R. L.; Fox, D. J.; Keith, T.; Al-Laham, M. A.; Peng, C. Y.; Nanayakkara, A.; Gonzalez, C.; Challacombe, M.; Gill, P. M. W.; Johnson, B. G.; Chen, W.; Wong, M. W.; Andres, J. L.; Head-Gordon, M.; Replogle, E. S.; Pople, J. A. *Gaussian 98*; Gaussian, Inc.: Pittsburgh, PA, 1998. (b) Foresman, J. B.; Head-Gordon, M.; Pople, J. A.; Frisch, M. J. *J. Phys. Chem.* **1992**, *96*, 135. (c) Johnson, B. G.; Gill, P. M. W.; Pople, J. A. *J. Chem. Phys.* **1993**, *98*, 5612.